Supporting Information

Electrocatalytic Efficiency Analysis of Catechol Molecules for NADH Oxidation during Nanoparticle Collision

Li-Jun Zhao, Ruo-Can Qian, Wei Ma, He Tian and Yi-Tao Long*

Key Laboratory for Advanced Materials and Department of Chemistry, School of Chemistry and Molecular Engineering, East China University of Science and Technology, 130 Meilong Road, Shanghai 200237, P. R. China. Fax: +86 21 64250032, E-mail: ytlong@ecust.edu.cn.

Contents

1. Materials and Reagents

All analytical grade reagents were purchased from Sigma-Aldrich. NADH was obtained from Sigma-Aldrich. UHQ II system (Elga) was used to purify water to a resistivity of 18 MΩ·cm for preparation of all solutions. Phosphate buffer solution (PBS) was prepared using Na_2HPO_4 and NaH_2PO_4 and deaerated by purging with nitrogen. All macroelectrodes for electrochemical experiment were purchased from Shanghai Chenhua Co., Ltd., China. All chemical reagents for synthesis were of analytical grade, obtained from commercial suppliers, and used without further purification unless otherwise noted. ^{1}H NMR and ^{13}C NMR were acquired in D_2O, MeOD, DMSO-d_6 or $CDCl_3$ on BRUKER AVANCE 500 spectrometer using TMS as an internal standard. HRMS were obtained on HP 5989 mass spectrometer.

2. Experimental Section

2.1 Synthesis and characterization of three thiol-catechol analogues 4-mercaptobenzene-1, 2-diol (CS1), N-(3, 4-dihydroxyphenethyl)-2-mercaptoacetamide (CS2) and N-(3, 4-dihydroxyphenethyl)-5-mercaptopentanamide (CS3)

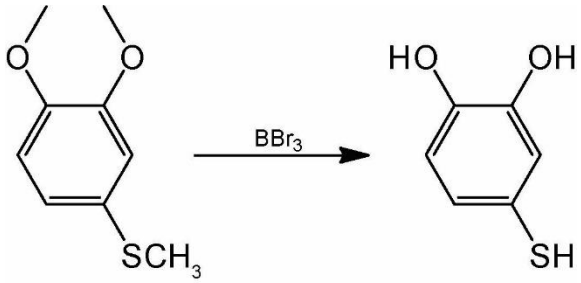

2a CS1

4-mercaptobenzene-1, 2-diol (CS1). Compound 1a (0.85 g, 5.0 mmol) was dissolved in dry dichloromethane (15 mL) and add to cooled to –10 ℃ under the nitrogen atmosphere. BBr_3 (2.50 g, 10 mmol) was added dropwise and then was stirred at –10 ℃ for 12 h. The mixture was quenched by ice water (20 mL) and stirred 2 h. The organic layer was washed with brine, dried over Na_2SO_4, filtered and evaporated. The residue was purified by silica gel column chromatography (10 % MeOH in DCM) to give compound CS1 as white solid (0.575 g, 81 %). ^{1}H NMR (400 MHz, MeOD): δ = 6.66 (d, J = 2.1 Hz, 1H), 6.59 (d, J = 8.3 Hz, 1H), 6.52 (m, J = 8.3, 2.2 Hz, 1H). ^{13}C NMR (101 MHz, D_2O): δ = 144.30, 142.55, 122.68, 119.96, 117.89, 116.73. 24.73. HRMS (EI): m / z calcd for (M^+) $C_6H_6O_2S$ 142.0090; found 142.0089.

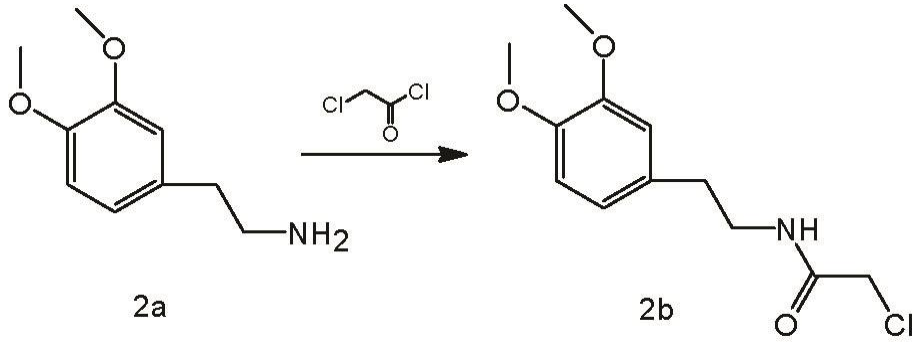

2a 2b

2-chloro-N-(3, 4-dimethoxyphenethyl) acetamide (2b). Compound 2a (3.62 g, 20 mmol) was dissolved in DCM (20 mL) was added triethylamine (6 mL). The mixture was cooled to 0 ℃ and stirred for 30 min. A solution of 2-chloroacetyl chloride (2.26 g, 30 mmol) in DCM (10 mL) was added to the above solution at 0 ℃ over 30 min, and then be transferred to room temperature for 4 h. The solution was filtered, and the filtrate was washed with brine, dried over Na_2SO_4, filtered and evaporated. The residue was purified by silica gel column chromatography (20 % EtOAc in PE) to give compound 2b as yellow oil (4.37 g, 85 %). ^{1}H NMR (400 MHz, $CDCl_3$): δ = 6.83 (d, *J* = 8.1 Hz, 1H), 6.77 – 6.71 (m, 2H), 6.64 (s, 1H), 4.03 (s, 2H), 3.88 (s, 3H), 3.87 (s, 3H), 3.55 (m, *J* = 13.0, 6.9 Hz, 2H), 2.80 (t, *J* = 7.0 Hz, 2H). ^{13}C NMR (101 MHz, $CDCl_3$): δ = 165.78, 149.09, 147.83, 130.84, 120.67, 111.85, 111.44, 55.92, 55.856, 42.76 (s), 41.09, 34.89.

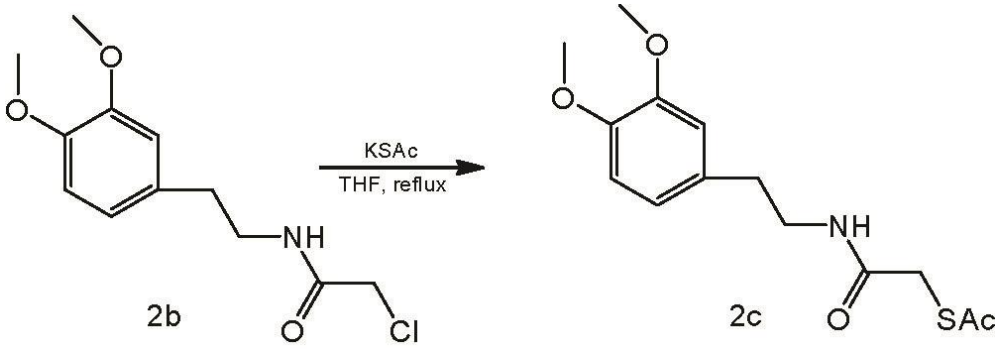

2b 2c

S-(2-((3, 4-dimethoxyphenethyl) amino)-2-oxoethyl) ethanethioate (2c). A solution of compound 2b (3.34 g, 13 mmol) and potassium thioacetate (1.63 g, 14.3 mmol) in anhydrous THF (20 mL) was heated at reflux temperature for 10 h under the nitrogen atmosphere. After cooling to room temperature, the solution was filtered. The filtrate was evaporated in vacuo, and the residue was purified by column chromatography to give pure product 2c (2.89 g, 75 %) as yellow solid. ^{1}H NMR (400 MHz, $CDCl_3$): δ = 6.81 (d, *J* = 8.5 Hz, 1H), 6.74 – 6.68 (m, 2H), 6.22 (s, 1H), 3.89(s, 3H), 3.86 (s, 3H), 3.54 – 3.41 (m, 4H), 2.75 (t, *J* = 7.0 Hz, 2H), 2.34 (s, 3H). ^{13}C NMR (101 MHz, $CDCl_3$): δ = 193.10, 165.49, 146.40, 145.11, 128.59, 118.11, 109.44, 108.77, 53.38,53.33, 38.48, 32.38, 30.44, 27.63.

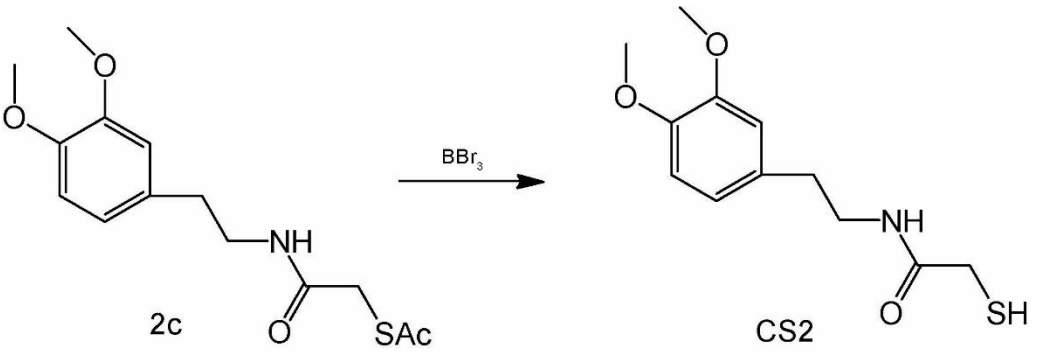

N-(3, 4-dihydroxyphenethyl)-2-mercaptoacetamide (CS2). Compound 2c (1.1 g, 3.7 mmol) was dissolved in dry dichloromethane (15 mL) and add to cooled to –10 ℃ under the nitrogen atmosphere. BBr_3 (2.0 g, 7.4 mmol) was added dropwise and then was stirred at –10 ℃ for 12 h, and then be transferred to room temperature for 4 h. The mixture was quenched by ice water (20 mL) and stirred 2 h. The organic layer was washed with brine, dried over Na_2SO_4, filtered and evaporated. The residue was purified by silica gel column chromatography (5 % MeOH in DCM) to give compound CS2 as yellow oil (0.604 g, 72 %). ^{1}H NMR (400 MHz, MeOD): δ = 6.81 – 6.42 (m, 3H), 4.87 (s, 4H), 3.35 (t, J = 7.4 Hz, 2H), 3.12 (s, 2H), 2.64 (t, J = 7.3 Hz, 2H). ^{13}C NMR (101 MHz, MeOD): δ = 171.75, 144.94, 143.40, 130.54, 119.83, 115.60, 115.11, 41.27, 34.34, 26.94. HRMS (ESI): m/z calcd for ($M+Na^+$) $C_{10}H_{13}NOSNa$ 250.0511; found 250.0514.

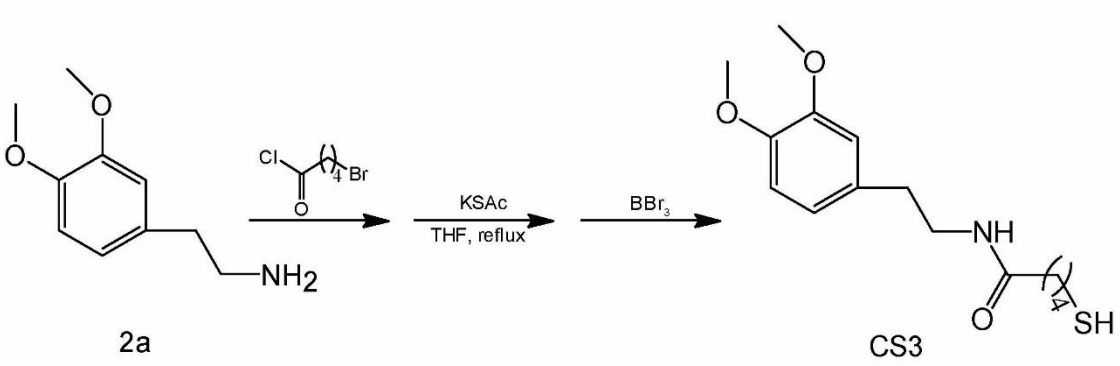

N-(3, 4-dihydroxyphenethyl)-5-mercaptopentanamide (CS3). The synthetic method of compound CS3 is similar to compound CS2. The different is the compound 2-chloroacetyl chloride replaced with compound 5-bromopentanoyl chloride. ^{1}H NMR (400 MHz, $CDCl_3$) δ 7.71 (s, 1H), 6.81 (d, J = 8.0 Hz, 1H), 6.74 (d, J = 2.0 Hz, 1H), 6.57 (m, J = 8.0, 2.0 Hz, 1H), 6.32 (s, 1H), 5.73 (t, J = 5.5 Hz, 1H), 3.50 – 3.45 (m, 1H), 2.70 (t, J = 7.0 Hz, 1H), 2.49 (m, J = 14.8, 7.1 Hz, 1H), 2.34 (s, 1H), 2.17 (t, J = 7.4 Hz, 1H), 1.72 – 1.65 (m, 1H), 1.57 (m, J = 7.7, 7.1, 4.2 Hz, 1H). ^{13}C-NMR (100MHz, CD_3OD, ppm): δ = 173.82, 144.27, 143.14, 130.55, 120.53, 115.50, 115.24, 40.98, 36.12, 34.87, 33.27, 24.34, 24.23. HRMS (ESI): m / z cacld for ($M+H^+$) $C_{13}H_{19}NO_3S$ 270.1160; found 270.1164.

2.2 Three thiol-catechol analogues CS1, CS2 and CS3-tagged AuNPs modified GC macroelectrodes and CV test for NADH oxidation.

AuNPs were modified with thiol-catechol analogues by mixing AuNPs colloid with 0.5 mM thiol-catechol analogues aqueous solution (0.5 mM) with a volume ratio of 1:1 for 12 h. It is necessary to wash AuNPs colloid with a sodium hydroxide solution (pH = 12) for twice before modified with thiol-catechol analogues, or the gold nanoparticles was easy aggregated. The obtained thiol-catechol analogues Au nanoparticles were washed with H_2O/t-BuOH (2 times), centrifuged, and finally redispersed in H_2O (1.5 mL). The thiol-catechol analogues tagged AuNPs were characterized by SERS, and the Raman characteristic lines of catechol were found at 1075 cm^{-1}.

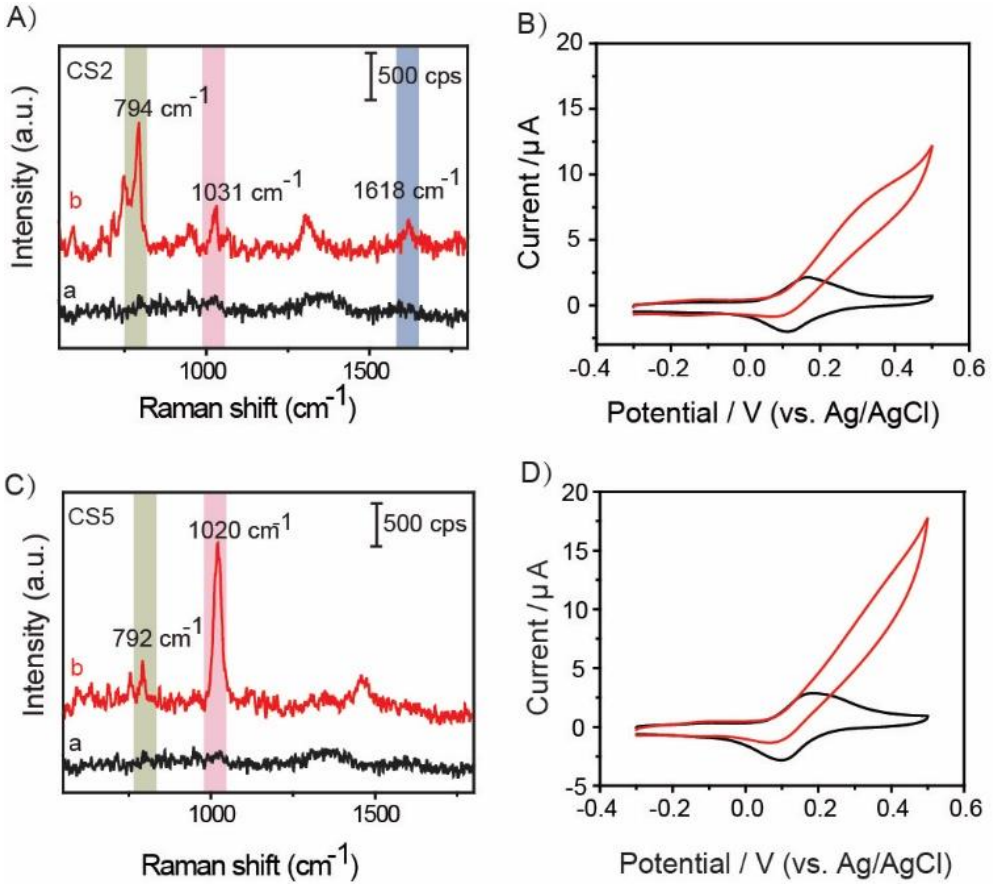

Figure S1. A) Raman spectrums of naked AuNPs (red line), CS2-tagged AuNPs (black line). B) CVs of CS2-tagged AuNPs modified GC electrodes with (red line) or without (black line) NADH (1 mM) at 100 mV/s; C) Raman spectrums of naked AuNPs (red line), CS3-tagged AuNPs (black line). D) CVs of CS3-tagged AuNPs modified GC electrodes with (red line) or without (black line) NADH (1 mM) at 100 mV/s.

Prior to each experiment, glassy carbon electrodes (3 mm) were polished with 1.0 μm diamond paste (Buehler) and rinsed with water and acetone. They were subsequently activated by placing them in a 1.0 M NaOH solution and holding the potential at +1.20 V for 5 min, followed by potential cycling from -0.200 to +1.00 V in 0.1 M phosphate buffer (pH 7.0) for 5 min. After rinsing, the electrodes were subsequently modified. To modify the GC electrode, 10 μL of the suspension of thiol-catechol analogues-capped AuNPs was drop-cast on the GC electrode and left to dry under a N_2 atmosphere.

2.3 Synthesis and characterization of 45 ±5 nm gold nanoparticles

Gold nanoparticles with average diameters of 14 nm were prepared by the citrate-mediated reduction of $HAuCl_4$. 50 mL of 0.01 wt % $HAuCl_4$ was heated to reflux with vigorous stirring and then 5 mL sodium citrate (38.8 mM) were added quickly to the solution. The mixed solution was continued to heat for 15 min, stopped heating and kept stirring for an additional 15 min. The resulting solution of colloidal particles was filtered and characterized by an absorption maximum at 518 nm using an ocean optical USB 2000+ UV-Vis spectrometer. Then, these particles were used as seed particles for the synthesis of 45 nm gold particles. To 25 mL of water, 1 mL of preformed seed gold particles and 100 μL of 0.2 M $NH_2OH·HCl$ was mixed. The mixture was stirred vigorously at room temperature and 3.0 mL of 0.1 wt % $HAuCl_4·3H_2O$ was added drop-wise. The size of Au nanoparticles was characterized by TEM.

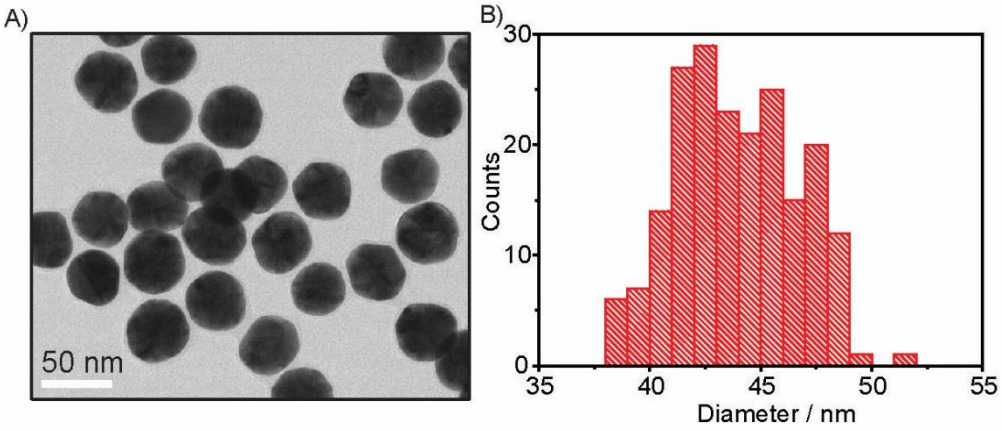

Figure S2. The transmission electron microscope (TEM) image (A) and size distribution (B) of 45 nm gold nanoparticles.

2.4 The electrochemistry oxidation of NADH on GC electrodes and naked AuNPs modified GC electrodes.

To show the good catalytic activity of CS1@AuNPs for NADH electrocatalytic oxidation was due to the CS1 shell, but not from the AuNPs. A control experiment was taken to compare the oxidation potential

and current of NADH with cleaning GC electrodes and bare AuNPs modified GC electrodes. An oxidation peak of NADH was observed at 0.780 V and the oxidation current is 22 μA with cleaning GC electrodes. Then, when a bare AuNPs modified GC electrode were used to conform same experiment, the oxidation potential shows nearly no change and the oxidation current have a slightly increase from 22 μA to 38 μA due to the increase of electrode surface areas.

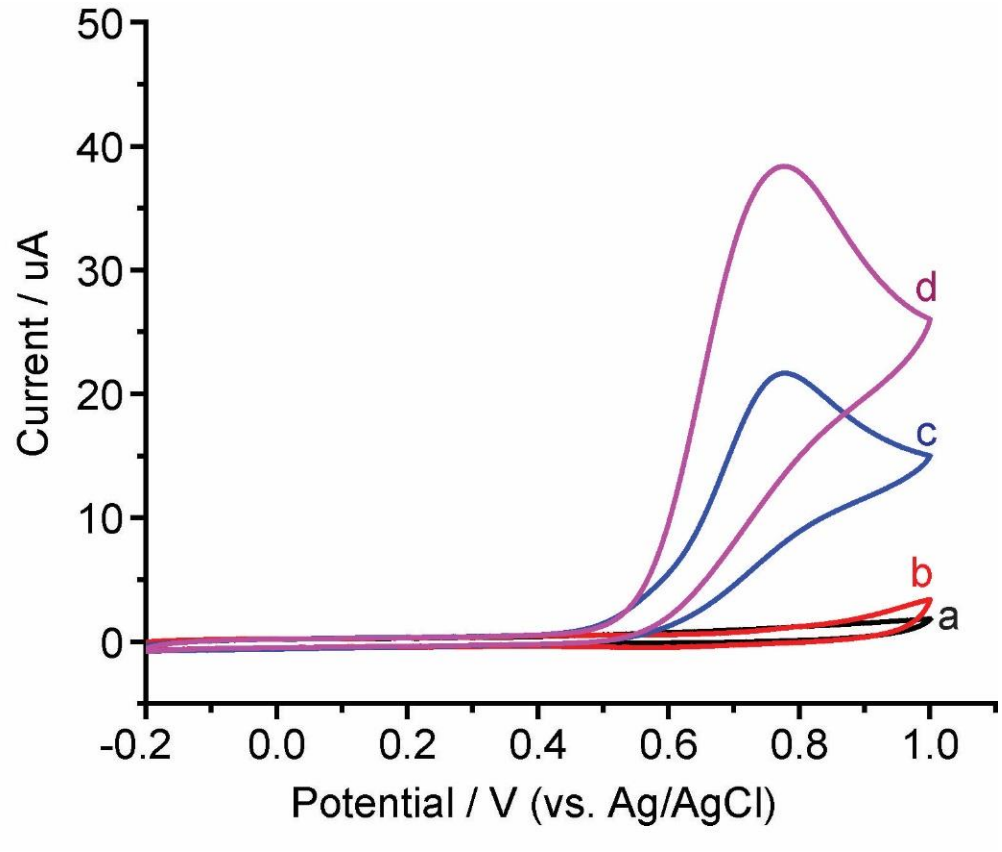

Figure S3. CVs of GC electrodes and bare AuNPs modified GC electrodes with (c, d) or without (a, b) of NADH (5 mM) at 100 mV s^{-1}. Bare AuNPs modified GC electrodes (b, d); clean GC electrodes (a, c).

2.5 The electrocatalytic effect of catechol for NADH oxidation in the absence of AuNPs

In order to investigate the electrocatalytic effect of catechol for NADH oxidation in the absence of AuNPs, cyclic voltammetry (CV) were performed on glassy carbon (GC) electrodes in 0.2 M PBS (pH 7.0); 0.2 M PBS (pH 7.0) containing 1 mM catechol; 0.2 M PBS (pH 7.0) containing 1 mM catechol and 1 mM NADH, respectively. When we compared the oxidation of catechol in 0.2 M PBS with and without NADH, a significantly enhancement of the anodic peak current was found to occur with NADH. The results indicated that catechol molecule have a good electrocatalytic effect for NADH oxidation.

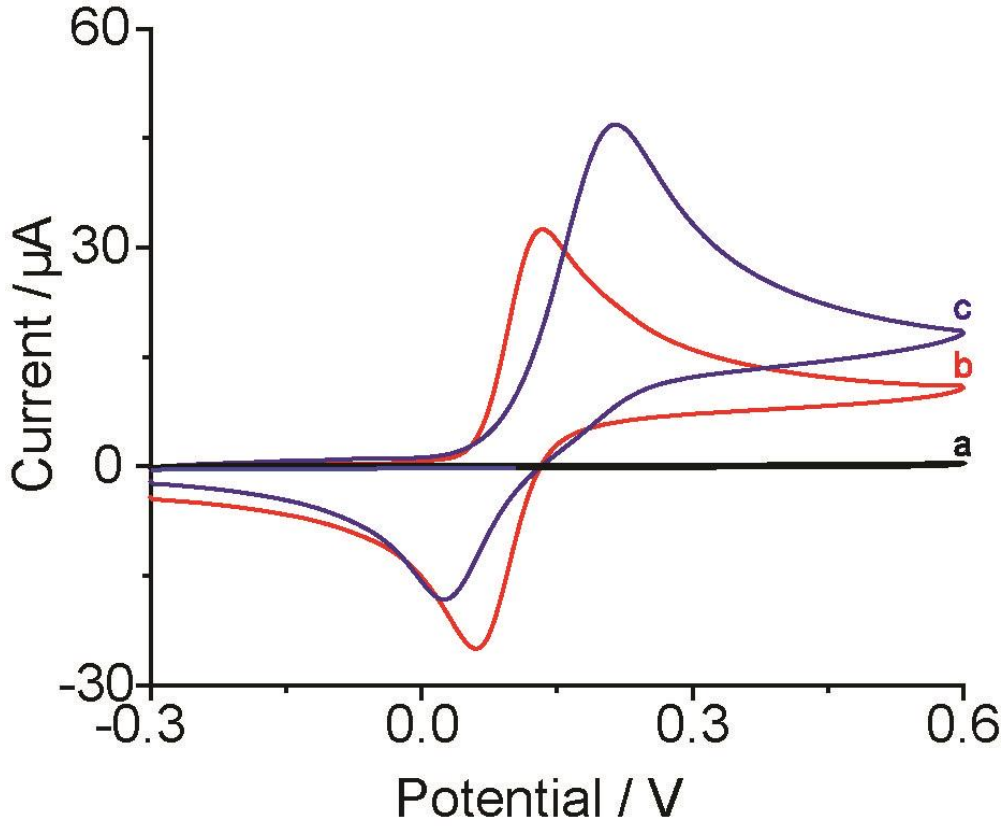

Figure S4. Cyclic voltammograms of: (a) glassy carbon electrode in 0.2 M PBS (pH 7.0); (b) cylic voltammograms of N glassy carbon electrode in in 0.2 M PBS (pH 7.0) in the presence of 1 mM catechol; (c) cylic voltammograms of glassy carbon electrode in 0.2 M PBS (pH 7.0) in the presence of 1 mM catechol and 5 mM NADH. Condition: scan rate of 100 mV s^{-1}.

2.6 Fabrication and characterization of carbon fiber UMEs

One end of the glass capillary was pulled by a heating coil puller (PP-2000, Narishige, Japan) and was sealed by a Bunsen lamp. A corn shape inside the pulled capillary favourably fitted the inserted carbon fiber to keep it straight. The carbon fiber was fixated and the electrode was sealed by dipping the pulled tip in a solution of epoxy (Epoxy Technology, Billerica, MA, U. S. A). Carbon-fiber UMEs were visually confirmed by dark-field microscopy. All the tip surfaces were polished in succession by polishing pads (Buehler Ltd., Bluff, Ilinois) coated with alumina having diameters of 3.5 μm, respectively. The glass sheath was sharpened by 3.0 and 0.05 μm diameter diamond pads. A used hard drive disk was used as polishing wheel, which was spun at high speed and had minor planer vibration.

The quality of these microelectrodes was monitored by cyclic voltammetry in 0.9 mM ferrocenylmethanol solution. In the cyclic voltammetry experiments, an electrochemical analyzer (CHI

660E, CH Instruments, Austin, Texas) was used. A two-electrode system was employed, where the UME was used as the working electrode, and a conventional Ag/AgCl electrode was served both as the reference and counter electrodes. Only electrode shows good reaction kinetics and stable steady-state currents, they could be used to the next experiments.

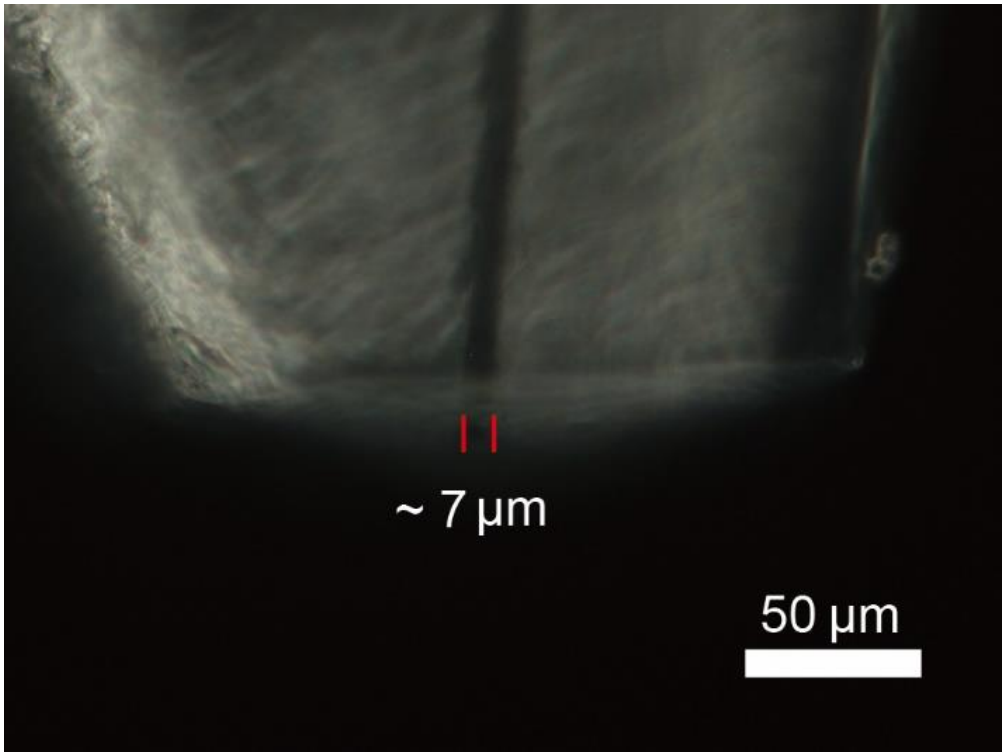

Figure S5. Microscopic image of carbon fiber UME.

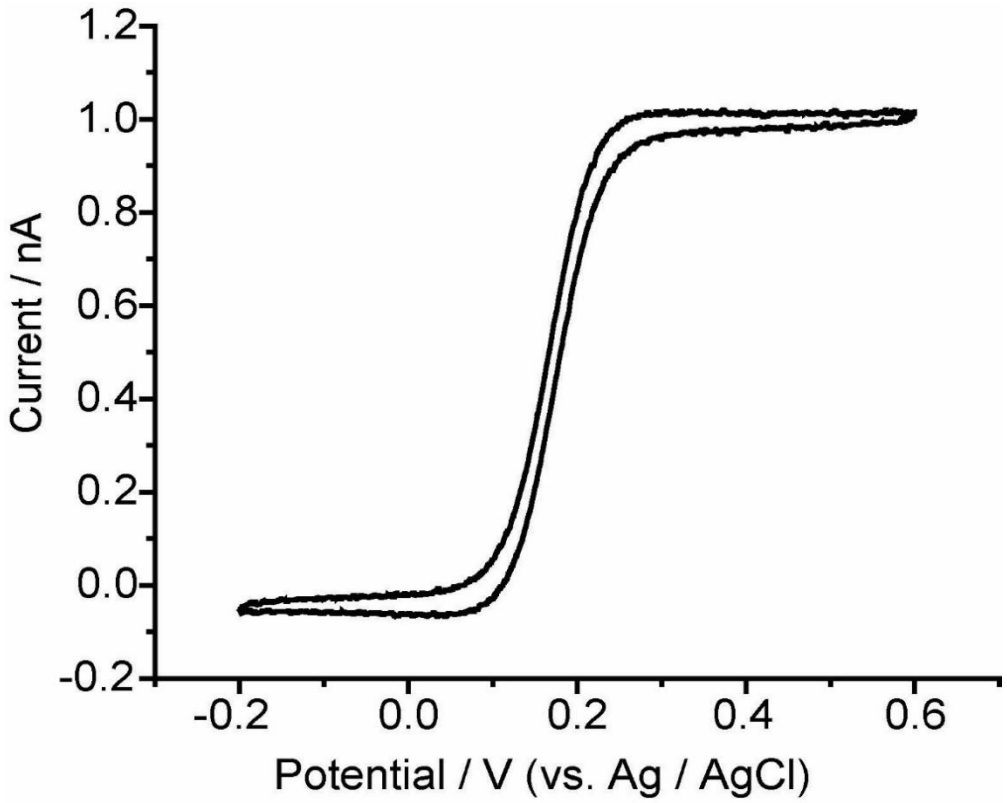

Figure S6. The CVs of carbon fiber microelectrode (7 μm in diameter) in 0.9 mM ferrocenylmethanol solution at 100 mV s^{-1}.

3. Collision Experiment Measurements and Data Processing

The electrochemical recording of CS1@AuNPs collision with ultramicroelectrode was performed by applying a constant potential of +700 mV (vs. Ag/AgCl) to the working electrode using a potentiostat (Axopatch 200B, Molecular Devices, Sunnyvale, CA, U.S.A.). The recorded signal was filtered at 1 kHz using a 4-pole Bessel filter and digitized at 25 kHz using a Digidata model 1440A with Axoscope 10.3 software (Axon Instruments Inc., Sunnyvale, CA, U.S.A.). All recorded data were analyzed by an in-house routine (can be provided upon request) written in MATLAB (R2013b, MathWorks Inc., Natick, MA, U.S.A.).

3.1 Chronoamperometric curves of single CS1@AuNP collisions at various potentials

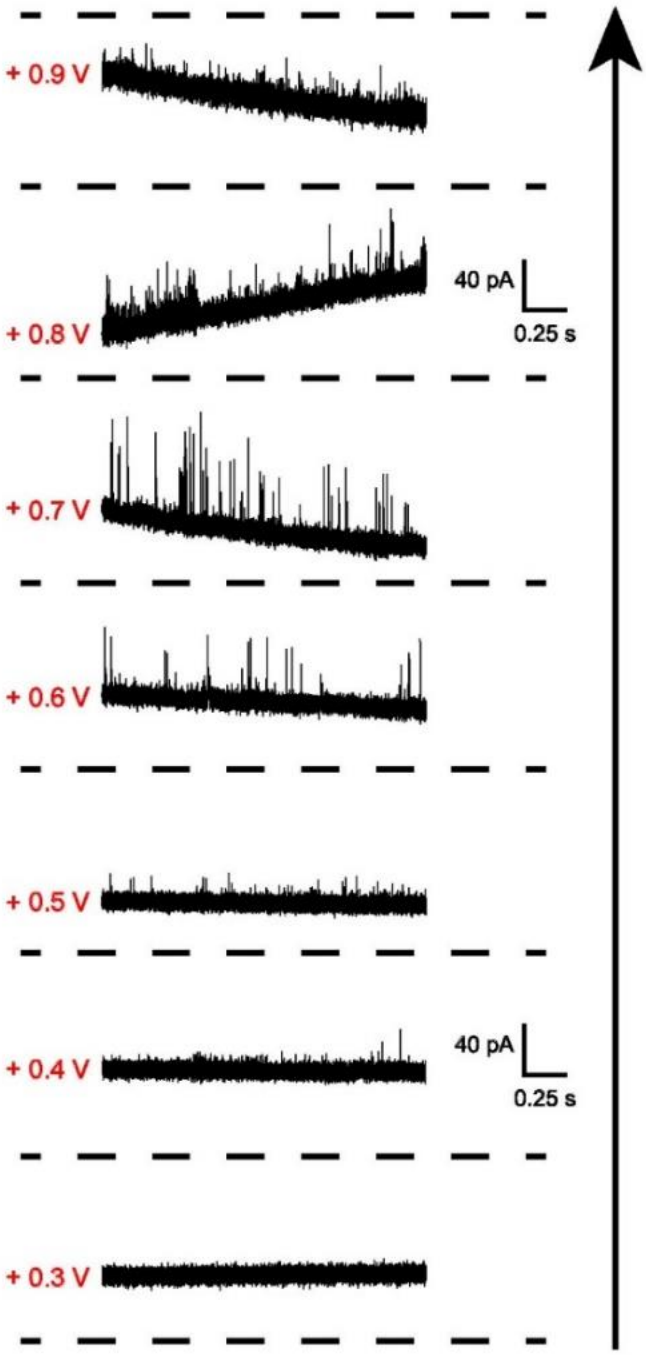

Figure S7. Chronoamperometric curves of single CS1@AuNP collisions at different applied potentials (0.3, 0.4, 0.5, 0.6, 0.7, 0.8 and 0.9 V) of Carbon-fiber UME in a 15 mM phosphate buffer (pH 7.0) containing 5 mM NADH. The CS1@AuNP concentration was 0.1 nM, and the data acquisition time was 2 s.

3.2 Impact of the filter frequency on the signal reading of the peak current spikes

We performed the single NP catalyzed experiments using 3 different filter frequencies, 1 KHz, 2KHz, 5KHz, respectively. As shown in Figure S7, a best signal-noise ratio was obtained at 5KHz. As the filter frequency decreased from 5 KHz to 1 KHz, the peak currents decreased evidently while the durations extended longer, leading to obvious changes on the shape of the current spikes.

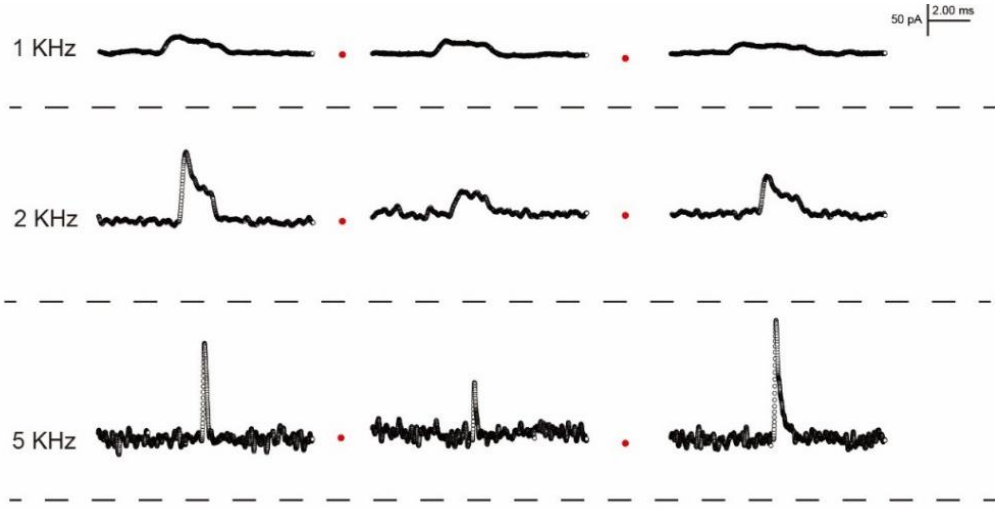

Figure S8 Chronoamperometric curves of single CS1@AuNP collisions on Carbon-fiber UME at different filter frequency (1 KHz, 2 KHz, 5 KHz) in 15 mM phosphate buffer (pH 7.0) containing 5 mM NADH. The CS1@AuNP concentration was 0.1 nM.

3.3 Amperometric traces of CS1@AuNP on the surface of UME before and after adding NADH

The chronoamperometric curves of carbon-fiber UME in PBS with CS1@AuNP before and after adding NADH was recorded, the background current was significantly increased when NADH was added, indicated that the increased background current was caused by NADH.

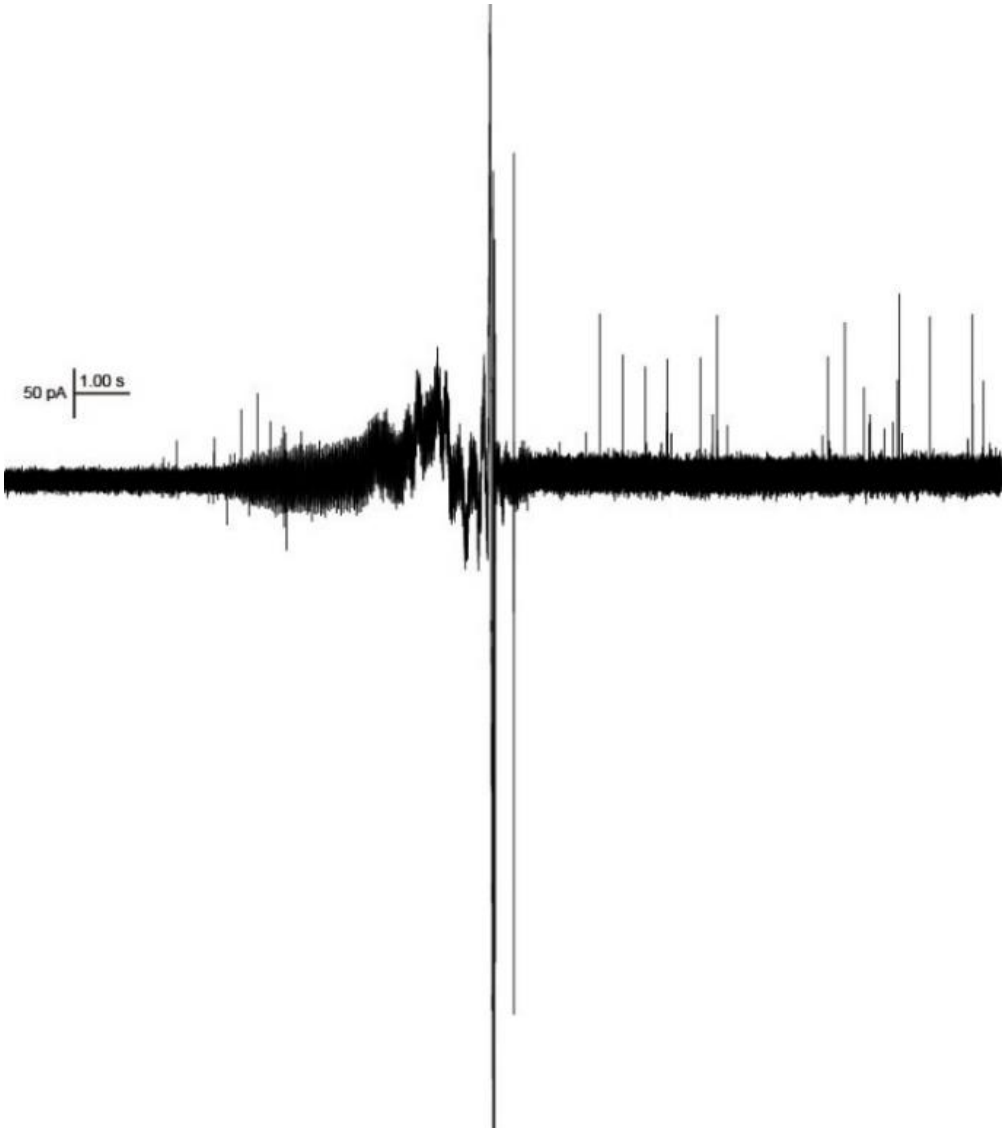

Figure S9. Chronoamperometric curves for carbon-fiber microelectrode in PBS (15 mM, pH = 7.0) with CS1@AuNP (100 pM) at 0.700 V before and after adding NADH (5 mM).

3.4 Amperometric traces of bare AuNPs on the surface of carbon fiber microelectrodes (UME)

To show the good catalytic activity of CS1 functional AuNPs for NADH electrocatalytic oxidation on the surface of carbon-fiber UME was due to the compound of CS1 but not the bare AuNPs, a control experiment was carried out with bare AuNPs in PBS (15 mM, pH = 7.0) with (A) or without (B) NADH.

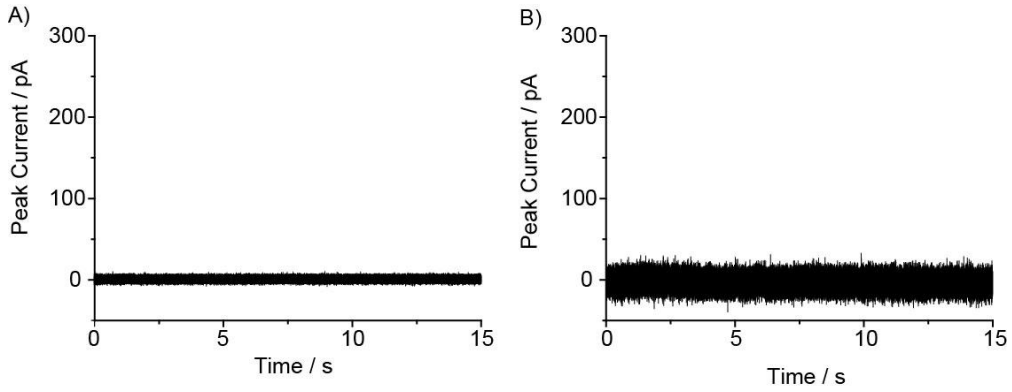

Figure S10. Chronoamperometric curves for carbon-fiber microelectrode in PBS (15 mM, pH = 7.0) with bare AuNP (100 pM) at 0.700 V in the absence (A) or presence (B) NADH (5 mM).

3.5 The number of CS1 molecules attached on the surface of a single AuNP

In order to evaluate the coverage of the smart shell, the number of CS1 molecules on the surfaces of a single AuNP (N_t) was calculated according to the equation (1):

$$N_t = \frac{f \times S}{S_t} \qquad (1)$$

with f being the fractional filling efficiency assuming optimal close-packing of tag molecules (0.91 for spheres on a plane); S being the surface area of the bare AuNP, S_t being the two-dimensional area occupied by a tag molecular. And the S_t can be estimated by the atomic size and the bond length of the CS1 molecule to be 9.81×10^{-20} m^2. The surface area of 45 nm AgNP can be estimated to be 6.36×10^{-15} m^2 by equation (2)

$$S = 4\pi r^2 \qquad (2).$$

Based on the above hypothesis, the N_t was calculated to be 5.9×10^4 on each AuNP of 45 nm.

4. The ^{1}H NMR, ^{13}C NMR and MS Characterization of Target Compounds and Intermediates

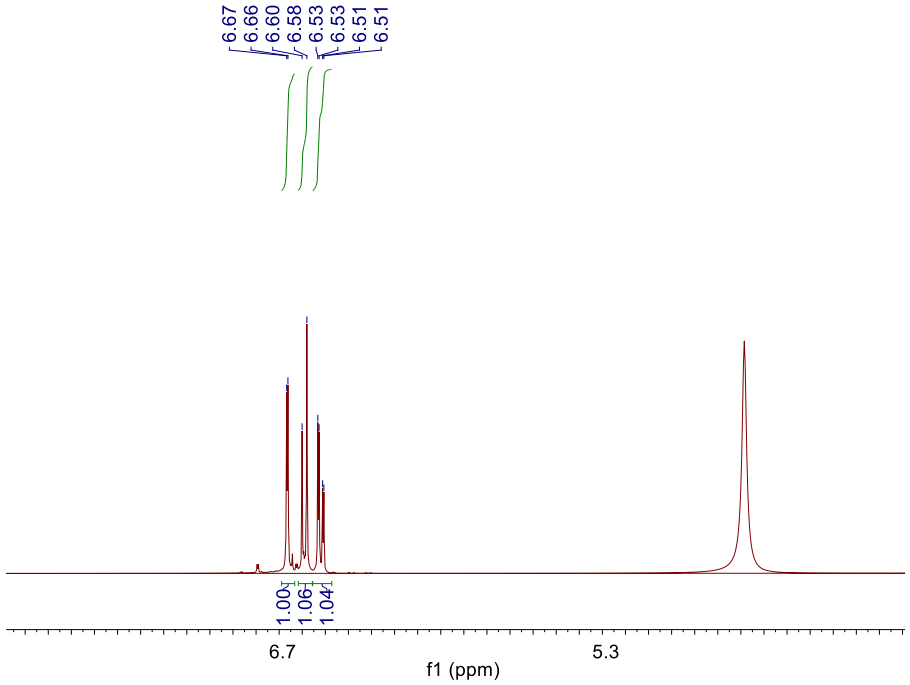

Figure S11. ^{1}H NMR spectrum of 4-mercaptobenzene-1, 2-diol (CS1)

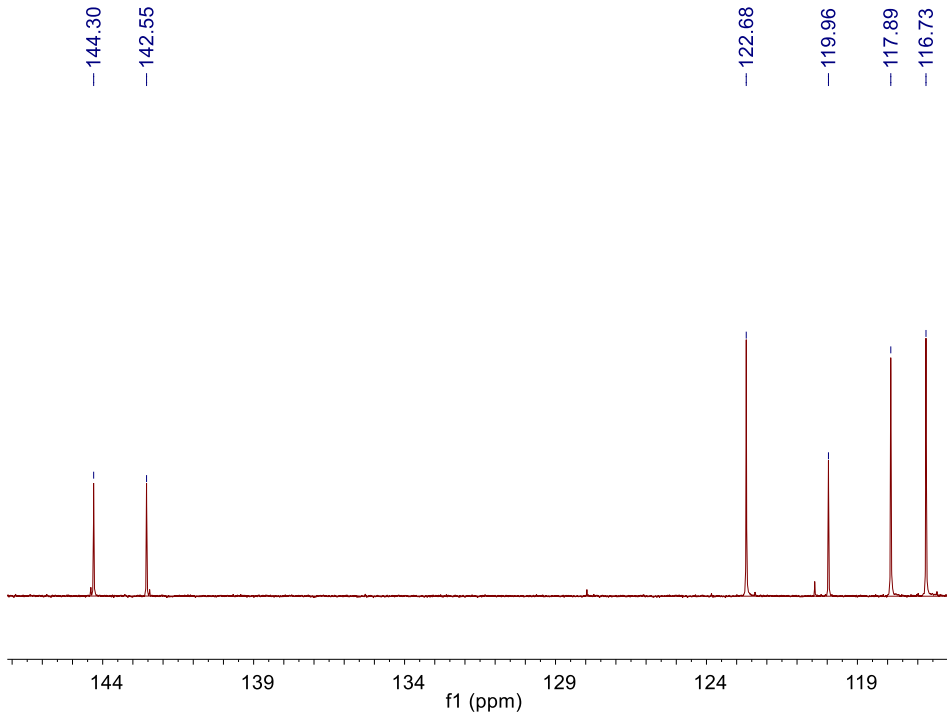

Figure S12. ^{13}C NMR spectrum of 4-mercaptobenzene-1, 2-diol (CS1)

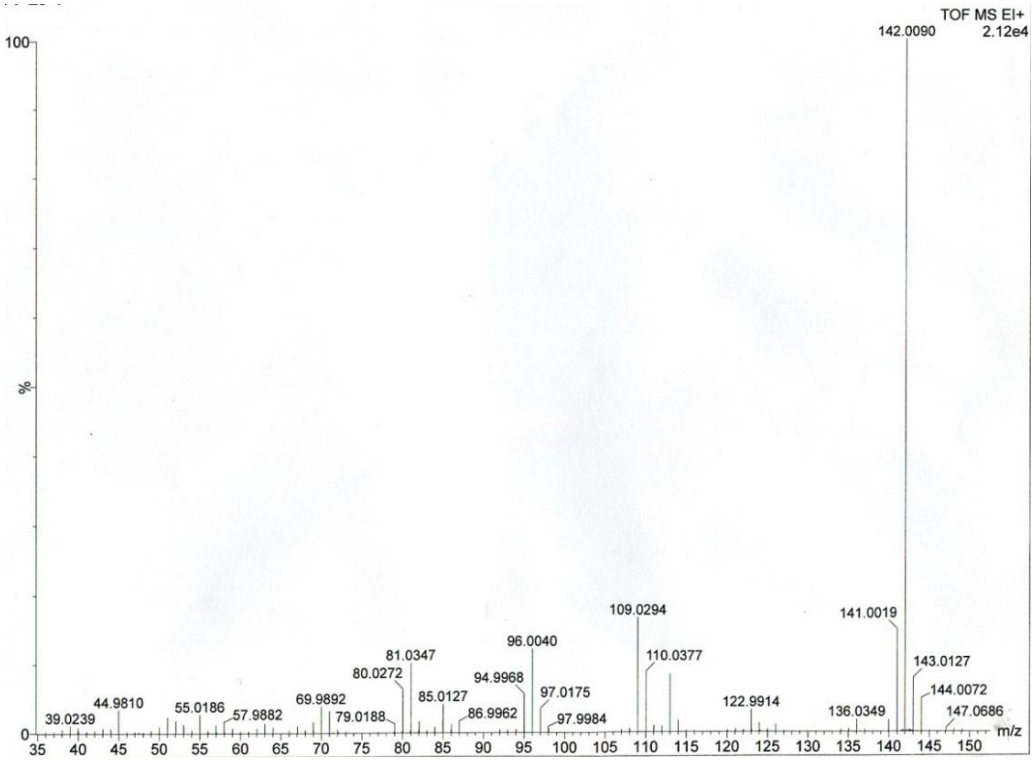

Figure S13. Mass spectrum of 4-mercaptobenzene-1, 2-diol (CS1)

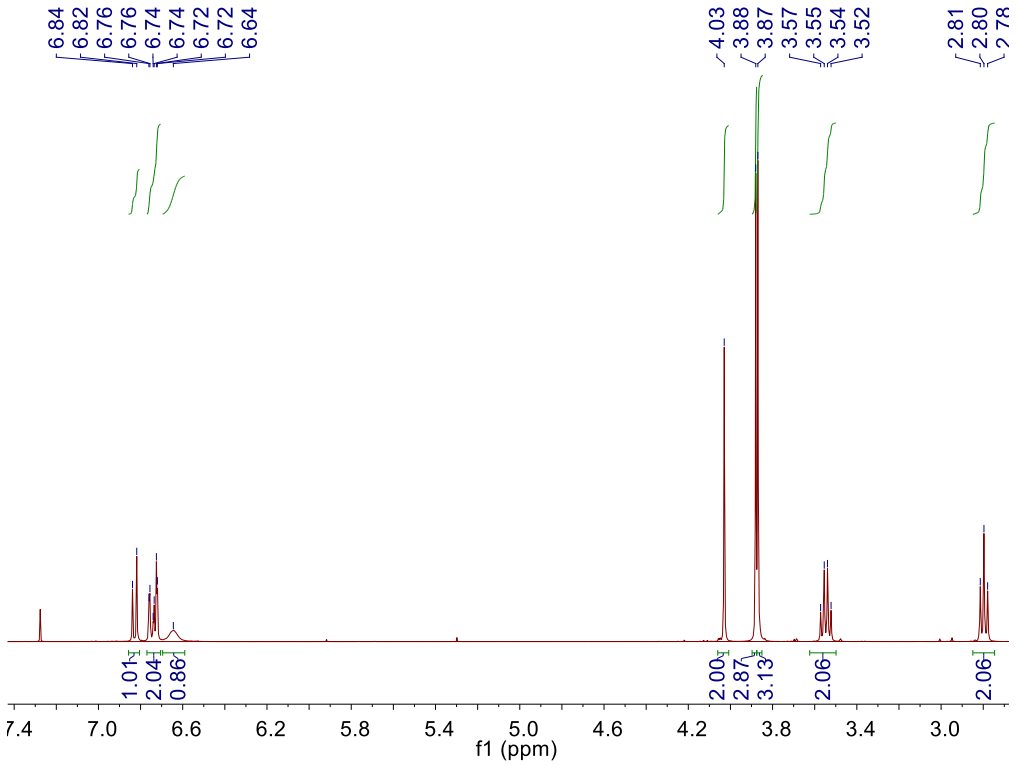

Figure S14. ^{1}H NMR spectrum of 2-chloro-N-(3, 4-dimethoxyphenethyl) acetamide (2b)

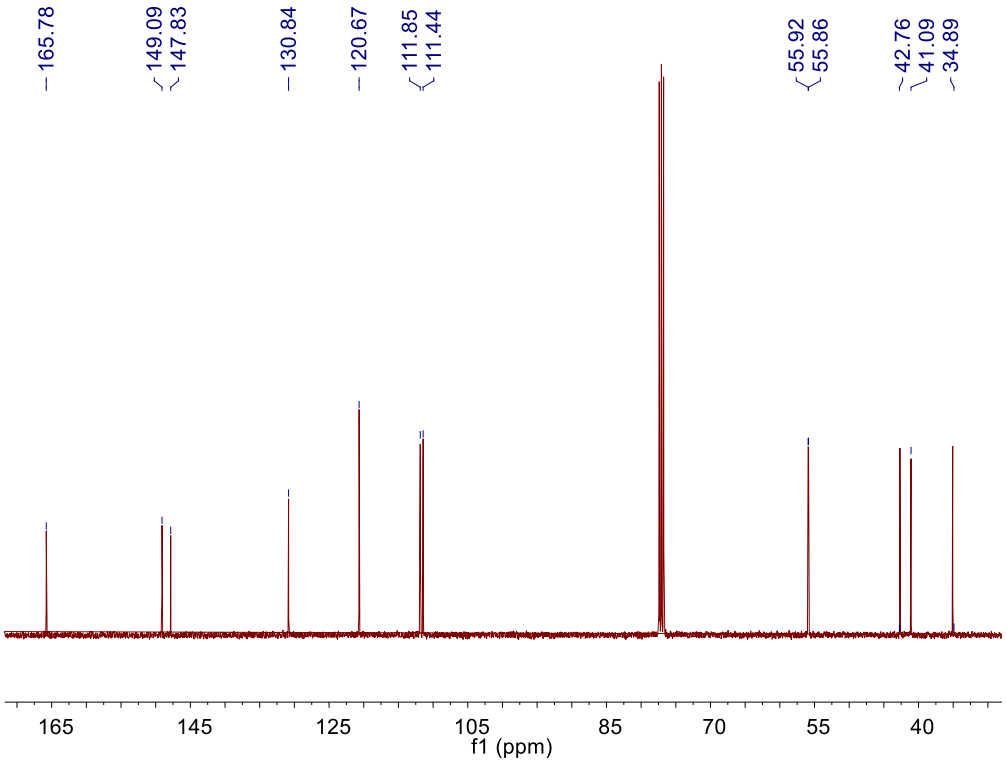

Figure S15. ^{13}C NMR spectrum of 2-chloro-N-(3, 4-dimethoxyphenethyl) acetamide (2b)

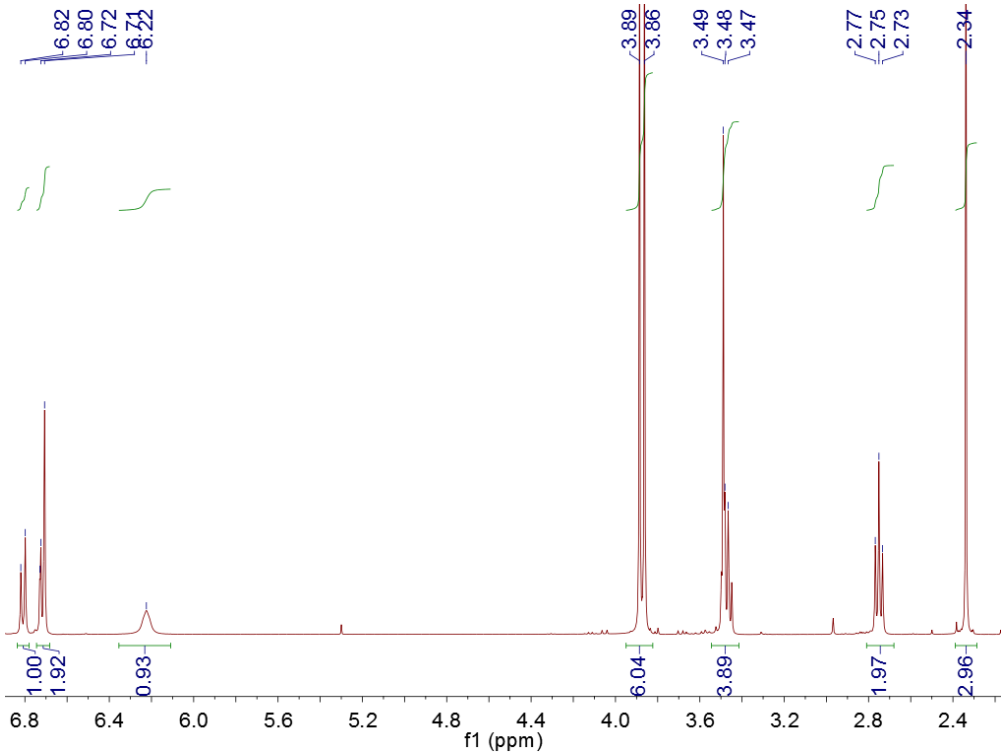

Figure S16. ^{1}H NMR spectrum of S-(2-((3, 4-dimethoxyphenethyl) amino)-2-oxoethyl) ethanethioate (2c)

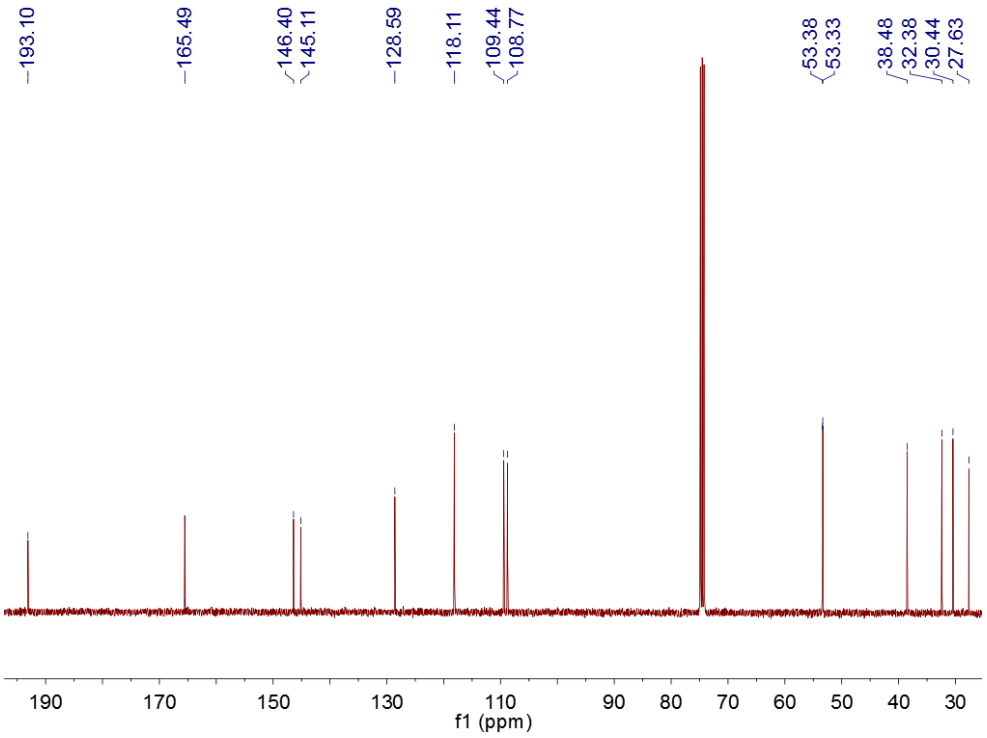

Figure S17. ^{13}C NMR spectrum of S-(2-((3, 4-dimethoxyphenethyl) amino)-2-oxoethyl) ethanethioate (2c)

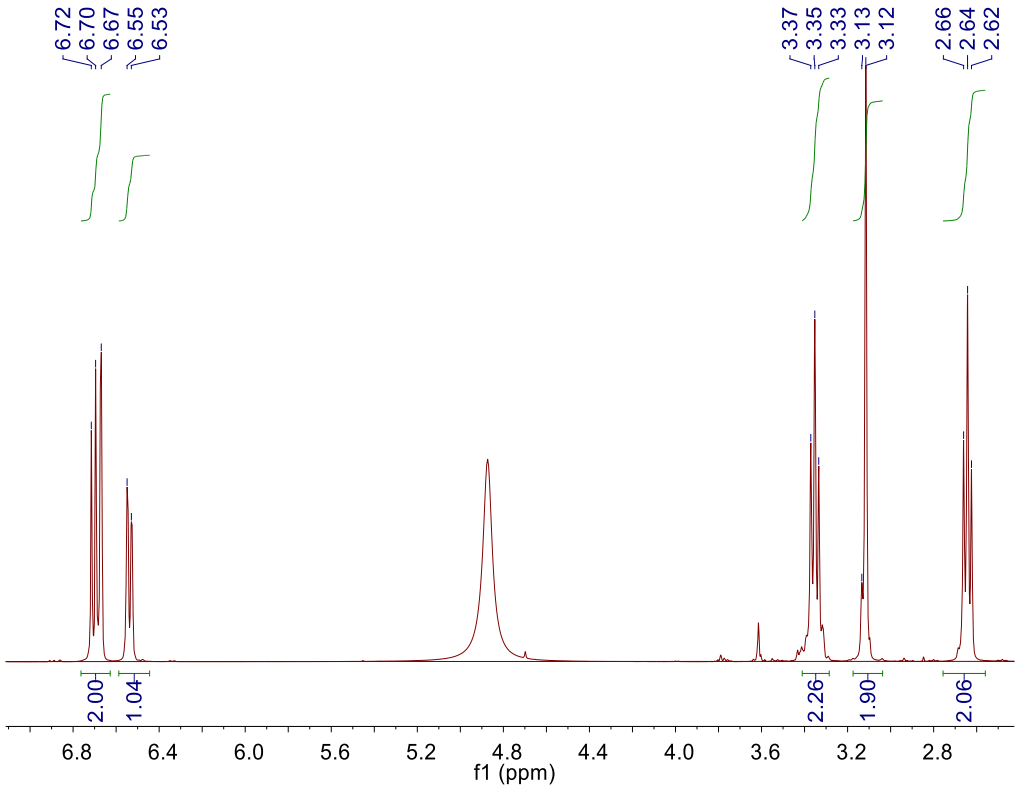

Figure S18. ^{1}H NMR spectrum of N-(3, 4-dihydroxyphenethyl)-2-mercaptoacetamide (CS2)

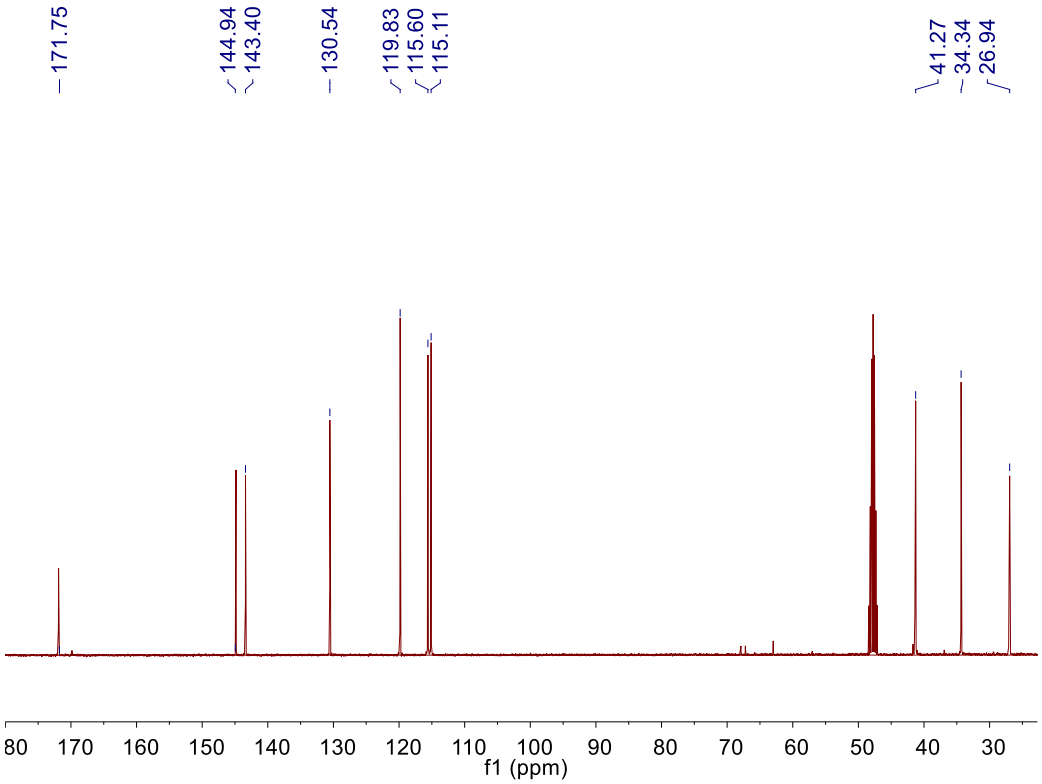

Figure S19. ^{13}C NMR spectrum of N-(3, 4-dihydroxyphenethyl)-2-mercaptoacetamide (CS2)

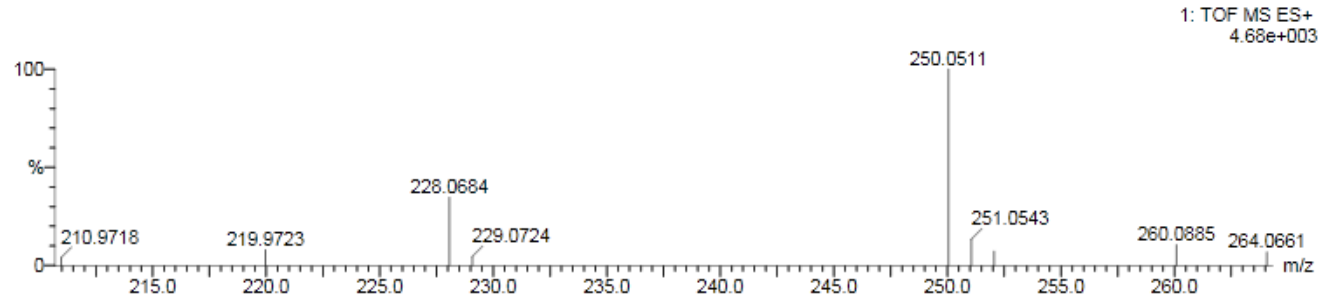

Minimum:				-1.5			
Maximum:		300.0	50.0	100.0			
Mass	Calc. Mass	mDa	PPM	DBE	i-FIT	i-FIT (Norm)	Formula
250.0511	250.0514	-0.3	-1.2	4.5	5.7	0.0	C10 H13 N O3 Na S

Figure S20. Mass spectrum of N-(3, 4-dihydroxyphenethyl)-2-mercaptoacetamide (CS2)

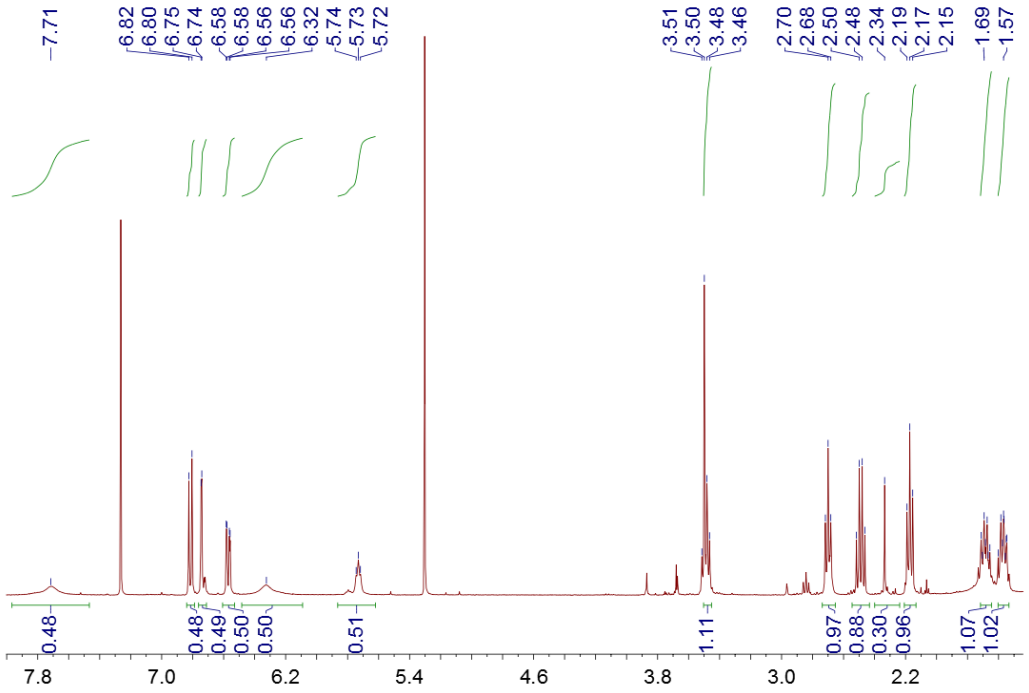

Figure S21. [1]H NMR spectrum of N-(3, 4-dihydroxyphenethyl)-5-mercaptopentanamide (CS3)

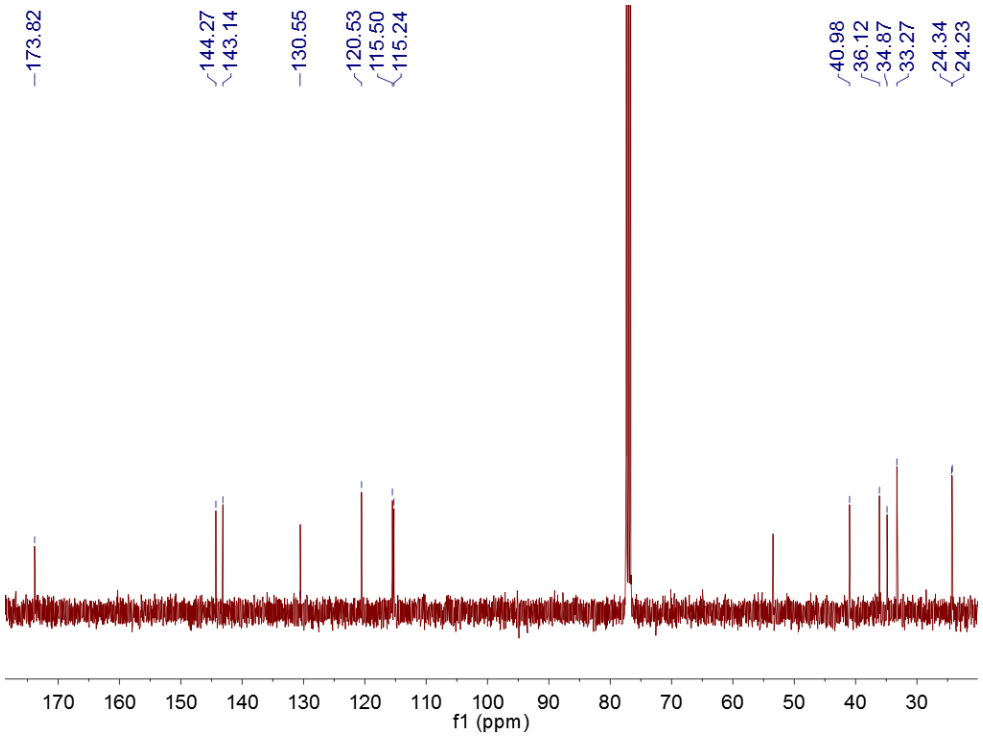

Figure S22. [13]C NMR spectrum of N-(3, 4-dihydroxyphenethyl)-5-mercaptopentanamide (CS3)

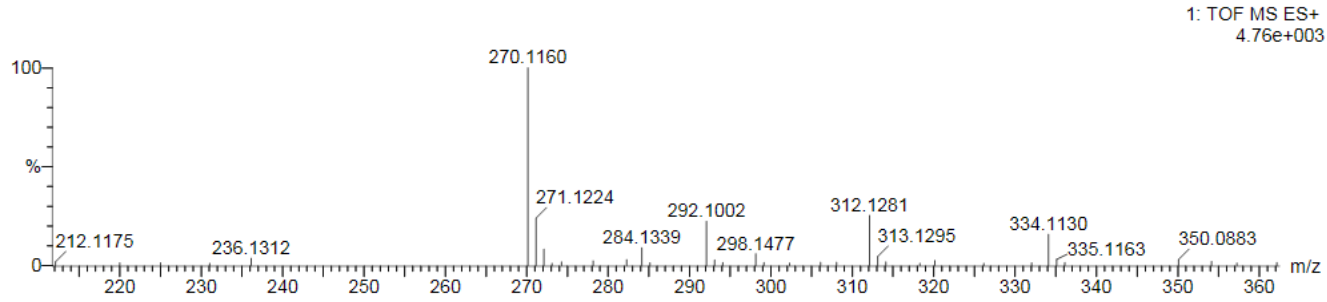

Minimum:				-1.5			
Maximum:		300.0	50.0	100.0			
Mass	Calc. Mass	mDa	PPM	DBE	i-FIT	i-FIT (Norm)	Formula
270.1160	270.1164	-0.4	-1.5	4.5	16.3	0.0	C13 H20 N O3 S

Figure S23. Mass spectrum of N-(3, 4-dihydroxyphenethyl)-5-mercaptopentanamide (CS3)